# Carbazole-Containing Conjugated Copolymers as Colorimetric/ Fluorimetric Sensor for Iodide Anion

**Muthalagu Vetrichelvan,[†] Rajagopal Nagarajan,[†] and Suresh Valiyaveettil*[,†,‡]**

*Singapore-MIT Alliance, E4-04-10, 4 Engineering Drive 3, Singapore-117576, and Department of Chemistry, National University of Singapore, 3 Science Drive 3, Singapore-117543*

*Received June 17, 2006; Revised Manuscript Received September 8, 2006*

ABSTRACT: A series of conjugated poly(*p*-phenylene carbazole) copolymers, poly(*N*-hexyl-3,6-carbazole-*alt*-2,5-bisdodecyloxyphenylene) [**P1**], poly(*N*-ethylhexyl-3,6-carbazole-*alt*-2,5-bisdodecyloxyphenylene) [**P2**], and poly(*N*-dodecyl-3,6-carbazole-*alt*-2,5-bisdodecyloxyphenylene) [**P3**] were prepared by using palladium-catalyzed Suzuki coupling reactions. All copolymers were characterized by means of FT-IR, GPC, $^1$H and $^{13}$C NMR, UV−vis, fluorescence spectroscopy, and X-ray powder diffraction patterns. All copolymers were soluble in common organic solvents, exhibited good thermal stability up to 390 °C, and showed UV−vis absorbance and fluorescence maxima around 328 and 394 nm, respectively. The polymers **P1**−**P3** differed in *N*-alkyl substitution, i.e., *n*-hexyl (for **P1**), *n*-ethylhexyl (for **P2**), and *n*-dodecyl (for **P3**) groups. In addition, a third monomer, 2,5-substituted pyridine for poly(*N*-ethylhexyl-3,6-carbazole-*co*-2,5-didodecyloxy phenylene-*co*-2,5-pyridine) (**P4**) and dialkylated fluorene for poly(*N*-ethylhexyl-3,6-carbazole-*co*-2,5-didodecyloxy phenylene-*co*-9,9′-dihexylfluorene) (**P5**) was incorporated into the copolymer **P2** to investigate the influence on their optical properties. The UV−vis and fluorescence maxima of **P4** and **P5** showed significant red shift in $\lambda_{max}$ by 29 and 19 nm and $\Delta\lambda_{em}$ of 38 and 21 nm, respectively as compared to the polymers **P1**−**P3**. The quantum efficiencies of these polymers (52−78%) were relatively higher and may have good applications in the fabrication of LEDs. The UV−vis and fluorescence spectra of the polymers were significantly affected by the addition of tetrabutylammonium iodide and other metal iodides. A colorless polymer solution turns to deep yellow color on the addition of iodide salts. This change is, however, not observed in the presence of other anions such as fluoride, chloride and bromide salts. Therefore, the polymers **P1**−**P5** may be useful in fabricating selective iodide sensors.

## Introduction

Conjugated polymers have received much attention due to their extended $\pi$-electron systems. Their potential applications includes light emitting diodes,[1−7] thin film transistors,[1,2] chemical sensors,[8] and electronic and photonic devices.[9−11] The optoelectronic properties of conjugated polymers vary significantly based on the degree of extended conjugation between the consecutive repeating units and the inherent electron densities on the polymer backbone.[12−14] Soft organic materials possess several advantages such as ease of processing and the tunability of their properties through chemical modifications.[15] Poly(vinylcarbazole) is known to be a good hole-transporting material.[16] Homopolymers of *n*-alkyl substituted 3,6-carbazole[17,18a−c] and its copolymers with thiophene,[18d] bithiophene,[18d] benzothiadazole,[18d,e] dialkylated fluorene,[18f−g] and pyridine[18h] have been reported as interesting optical materials. The optical properties and solvatochromism of homopolymers and copolymers of *n*-alkyl-substituted 2,7-carbazole were extensively investigated by the Leclerc group.[16,19]

The carbazole is an interesting functional group for incorporation on to polymer backbone owing to its higher thermal stability, solubility, extended glassy state and moderately high oxidation potential.[20−24] In addition, it is well-known that the carbazole containing oligomers and conjugated polymers are good hole-transport materials.[18g,25−27] Our research efforts are focused on the synthesis and structure−property investigations of asymmetrically functionalized, planar conjugated polymers.[28−33]

The synthesis of alternating copolymers containing electron-rich *n*-alkyl-3,6-substituted carbazoles and dialkoxybenzene systems are described with full details. In addition, a third monomer, using pyridine and alkylated fluorene moieties, was also introduced on the copolymer backbone in order to enhance electron affinity and reduce the band gap of these copolymers. The syntheses, characterization and optical properties of poly(*N*-hexyl-3,6-carbazole-*alt*-2,5-bisdodecyloxy phenylene) [**P1**], poly(*N*-ethylhexyl-3,6-carbazole-*alt*-2,5-bisdodecyloxy phenylene) [**P2**], poly(*N*-dodecyl-3,6-carbazole-*alt*-2,5-bisdodecyloxy phenylene) [**P3**], poly(*N*-ethylhexyl-3,6-carbazole-*co*-2,5-bisdodecyloxy phenylene-*co*-2,5-pyridine) [**P4**], and poly(*N*-ethylhexyl-3,6-carbazole-*co*-2,5-bisdodecyloxy phenylene-*co*-9,9′-dihexylfluorene) [**P5**] were investigated in detail (Scheme 1). The *N*-alkyl groups and dodecyloxy groups incorporated on polymer backbone to increase the solubility and ordered packing through alkyl chain crystallization.

## Experimental Section

**Chemicals and Instrumentation**: All reagents were purchased from commercial sources and used without further purification unless otherwise stated. All reactions were carried out under inert atmosphere ($N_2$ or Ar) using freshly distilled anhydrous solvents. Tetrahydrofuran (THF) was purified by distillation over sodium under nitrogen atmosphere. The $^1$H and $^{13}$C NMR spectra were collected on a Bruker ACF 300 spectrometer operating at 300 and 75.5 MHz, respectively. Chloroform-*d* was used as solvent and tetramethylsilane as internal standard. FT-IR spectra were recorded on a Bio-Rad FTS 165 spectrophotometer using KBr as matrix. A UV−vis spectra was recorded using a Shimadzu 3101 PC spectrophotometer and fluorescence measurements were made on a RF-5301PC Shimadzu spectrofluorophotometer. All spectra were recorded in chloroform. Thermogravimetric analyses were done using TA Instruments SDT 2960 with a heating rate of 10 °C/min

* To whom correspondence should be addressed at the Department of Chemistry, National University of Singapore. Telephone: (65) 6516 4327. Fax: (65) 6779 1691. E-mail: chmsv@nus.edu.sg.
[†] Singapore-MIT Alliance.
[‡] Department of Chemistry, National University of Singapore.

10.1021/ma0613537 CCC: $33.50 
Published on Web 11/04/2006

**Scheme 1. Molecular Structures of Polymers, P1−P5**

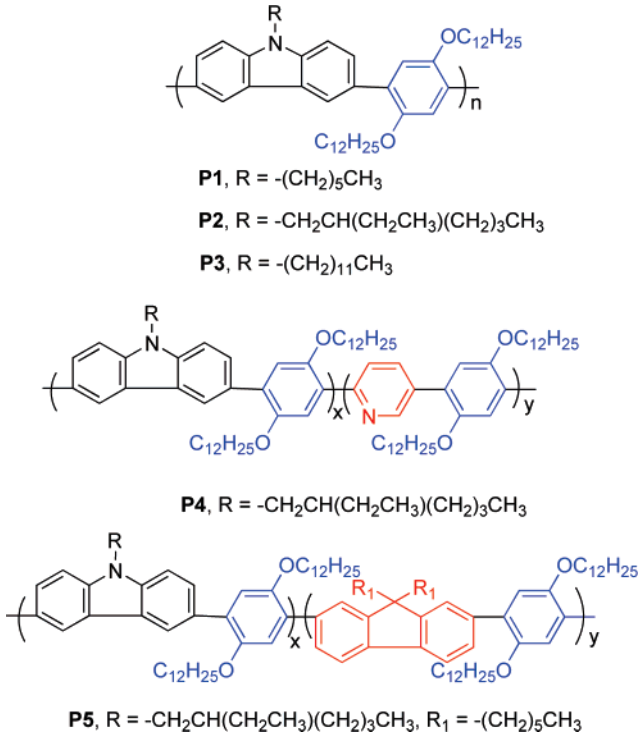


under nitrogen atmosphere. Differential scanning calorimetry (DSC) measurements were done on TA Instruments DSC 2960 at a heating rate of 20 °C/min. Gel permeation chromatography (GPC) was used to obtain the molecular weight of the polymers with reference to polystyrene standards with THF as eluant. X-ray powder patterns were obtained using a D5005 Siemens X-ray diffractometer with Cu Kα (1.54 Å) radiation (40 kV, 40 mA). Samples were mounted on a sample holder and scanned between $2\theta = 1.5$ and 40° with a step size of 0.01°.

**Synthesis**: Synthetic scheme for polymers **P1**−**P3** and **P4**−**P5** are shown in Schemes 2 and 3, respectively. 2,5-Dibromohydroquinone (**2**), 2,5-dibromo-1,4-bis(dodecyloxybenzene) (**3**), and 1,4-bis(dodecyloxy phenyl)-2,5-diboronic acid (**4**) were synthesized using the standard procedure reported in the literature.[28,34]

**General Procedure for the Synthesis of Polymers P1, P2, and P3.** Compound **4** (3.05 g, 5.7 mmol) and the *N*-alkylated dibromocarbazole **7** (5.7 mmol) were dissolved in dry THF (70 mL) under nitrogen atmosphere. After the addition of 2 M solution of $K_2CO_3$ (100 mL), the catalyst tetrakis(triphenylphosphino)palladium(0) (0.20 g, 3 mol %) and cetyltriethylammonium bromide (CTAB) (0.9 g, 40 mol %) were added and the mixture stirred vigorously for 4 days at 70−80 °C, cooled to room temperature and poured into 1 L of methanol. The black residue separated from the aqueous solution was extracted with large excess of chloroform, washed with water, dried with $MgSO_4$, filtered, and concentrated. The polymer was then redissolved in chloroform and precipitated from a large excess of methanol. The black glassy polymers obtained were washed with water followed by methanol (2 × 25 mL) and acetone (3 × 25 mL).

**P1:** Glassy black crystalline solid. Yield: 60%. $^1$H NMR ($CDCl_3$, $\delta$, ppm): 8.42 (s, 2H, Car−H), 7.78 (d, 2H, Car−H), 7.48 (d, 2H, Car−H), 7.26 (m, 2H, Ar−H), 4.37 (b, 2H, Car−NC**H**$_2$−), 3.99 (b, 4H, ArOC**H**$_2$−), 1.96 (b, 2H, CarNCH$_2$C**H**$_2$−), 1.71 (b, 4H, ArOCH$_2$**CH**$_2$−), 1.36−1.16 (b, 42H, −CH$_2$(**CH**$_2$)$_9$CH$_3$ and −N-(CH$_2$)$_2$(**CH**$_2$)$_3$CH$_3$), 0.90 (b, 9H, −**CH**$_3$). $^{13}$C NMR ($CDCl_3$, $\delta$, ppm): 150.6, 139.8, 132.1, 131.2, 129.3, 128.2, 127.5, 123.0, 121.2, 117.2, 107.9, 69.9, 43.3, 31.8, 31.6, 30.8, 29.5, 29.3, 29.0, 27.0, 26.1, 22.6, 14.0. FT-IR (KBr, cm$^{-1}$): 3436, 3229, 3053, 2921, 2852, 2031, 1603, 1512, 1479, 1379, 1294, 1200, 1153, 1043, 866, 804, 719, 695, 637. Anal. Calcd for $(C_{48}H_{71}NO_2)_n$: C, 83.00; H, 10.31; N, 2.01. Found: C, 82.63; H, 10.06; N, 2.12.

**Scheme 2. Synthesis of Polymers P1−P3**[a]

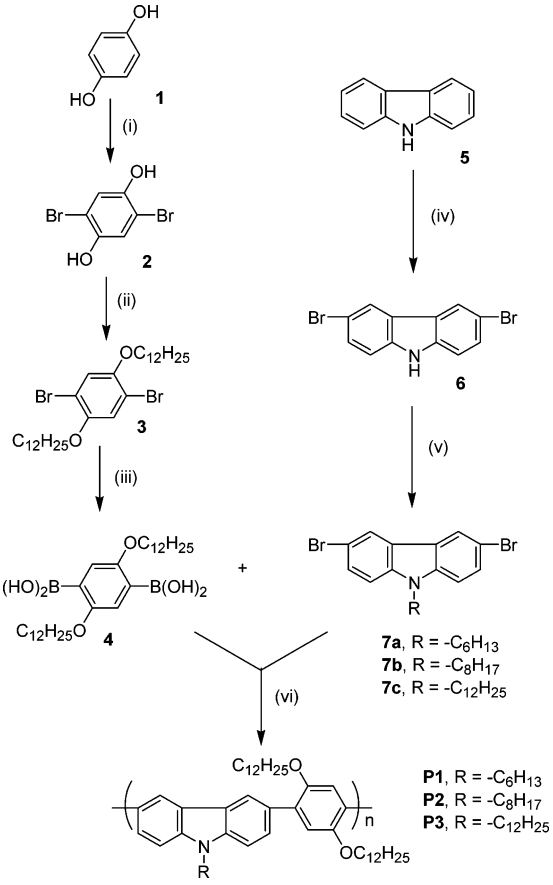


[a] Key: (i) $Br_2$/AcOH, 80%; (ii) NaOH, $CH_3(CH_2)_{11}Br$, 70 °C, 12 h, 75%; (iii) *n*-BuLi, THF, −78°C, triisopropyl borate, RT, 10 h, 70%; (iv) NBS/DMF, 80%; (v) KOH, RBr, THF, reflux, 2h; 85% (vi) $K_2CO_3$, THF, 3.0 mol % $Pd(PPh_3)_4$, CTAB, reflux, 4 d.

**P2:** Glassy black crystalline solid. Yield: 75%. $^1$H NMR ($CDCl_3$, $\delta$, ppm): 8.41 (s, 2H, Car−H), 7.79 (d, 2H, Car−H), 7.45 (d, 2H, Car−H), 7.26 (m, 2H, Ar−H), 4.24 (b, 2H, Car−NC**H**$_2$−), 3.99 (b, 4H, ArOC**H**$_2$−), 1.72 (b, 4H, ArOCH$_2$**CH**$_2$−), 1.36−1.16 (b, 45H, −CH$_2$(**CH**$_2$)$_9$CH$_3$ and −N(CH$_2$C**H**(CH$_3$)(**CH**$_2$)$_4$CH$_3$), 0.91−0.80 (m, 12H, −**CH**$_3$). $^{13}$C NMR ($CDCl_3$, $\delta$, ppm): 150.6, 140.4, 131.2, 129.3, 127.8, 127.5, 123.0, 121.1, 117.2, 108.2, 69.9, 47.6, 39.5, 31.8, 31.0, 29.3, 28.8, 26.1, 24.4, 23.0, 22.6, 14.0, 10.8. FT-IR (KBr, cm$^{-1}$): 3424, 3223, 3053, 2923, 2852, 1601, 1512, 1477, 1381, 1291, 1195, 1152, 1043, 866, 802, 720, 695, 637. Anal. Calcd for $(C_{50}H_{75}NO_2)_n$: C, 83.16; H, 10.47; N, 1.94. Found: C, 83.10; H, 11.08; N, 1.92.

**P3:** Black solid. Yield: 67%. $^1$H NMR ($CDCl_3$, $\delta$, ppm): 8.41 (s, 2H, Car−H), 7.78 (d, 2H, Car−H), 7.48 (d, 2H, Car−H), 7.26 (m, 2H, Ar−H), 4.35 (b, 2H, Car−NC**H**$_2$−), 3.98 (b, 4H, ArOC**H**$_2$−), 1.94 (b, 2H, Car−NCH$_2$C**H**$_2$−), 1.71 (b, 4H, ArOCH$_2$**CH**$_2$−), 1.30−1.16 (b, 54H, −CH$_2$(**CH**$_2$)$_9$CH$_3$ and −N-(CH$_2$)$_2$(**CH**$_2$)$_9$CH$_3$), 0.90 (b, 6H, −**CH**$_3$). $^{13}$C NMR ($CDCl_3$, $\delta$, ppm): 150.6, 139.8, 132.1, 128.4, 128.2, 122.9, 117.1, 110.9, 107.9, 69.9, 31.8, 29.5, 29.2, 27.3, 26.1, 22.6, 14.0. FT-IR (KBr, cm$^{-1}$): 3426, 3055, 2925, 2851, 1597, 1512, 1477, 1379, 1292, 1154, 1045, 866, 804, 719, 695, 637. Anal. Calcd for $(C_{54}H_{83}NO_2)_n$: C, 83.34; H, 10.75; N, 1.80. Found: C, 81.03; H, 10.30; N, 1.90.

**General Procedure for the Synthesis of Polymers, P4 and P5.** Compound **4** (6 mmol), *N*-alkylated dibromo carbazole (**7b**) (3 mmol) and 2,5-dibromo pyridine (**8**) or alkylated dibromofluorene **9** (3 mmol) were dissolved in dry THF (70 mL) under nitrogen atmosphere. The remaining synthetic procedure was same as for polymers **P1**−**P3** (see above).

**P4:** Pale greenish-black solid. Yield: 70%. $^1$H NMR ($CDCl_3$, $\delta$, ppm): 8.98 (b, 1H, py−H), 8.40 (s, 2H, Car−H), 8.10 (b, 2H, py−H), 7.76 (d, 2H, Car−H), 7.47 (d, 2H, Car−H), 7.11 (m, 2H,

**Scheme 3. Synthesis of Polymers P4 and P5**[a]

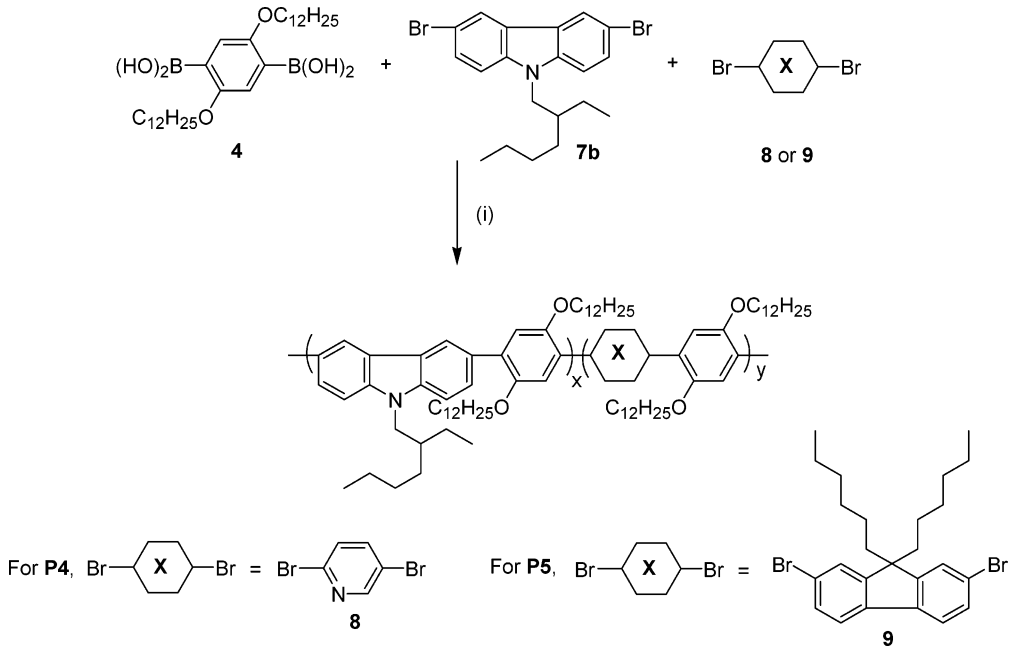


[a] Key: (i) $K_2CO_3$, THF, 3.0 Mol % $Pd(PPh_3)_4$, CTAB, reflux, 4 d.

Ar−H), 4.30−3.99 (m, 6H, Car−NC**H**$_2$− and ArOC**H**$_2$−), 2.10 (b, 2H, CarNCH$_2$C**H**$_2$−), 1.78 (b, 4H, ArOCH$_2$**CH**$_2$−), 1.50−1.16 (b, 79H, −CH$_2$**(CH**$_2$**)**$_9$CH$_3$, −NCH$_2$C**H**(CH$_3$)(**CH**$_2$)$_3$CH$_3$), 0.87 (b, 9H, −**CH**$_3$). $^{13}$C NMR ($CDCl_3$, $\delta$, ppm): 150.6, 149.4, 140.4, 136.3, 132.2, 131.6, 129.2, 128.4, 128.2, 124.4, 124.2, 123.0, 121.1, 115.6, 115.3, 69.8, 69.4, 31.8, 31.6, 30.9, 29.5, 29.3, 28.8, 26.1, 24.4, 23.0, 14.0, 10.8. FT-IR (KBr, cm$^{-1}$): 3424, 3055, 2921, 2851, 2361, 2028, 1548, 1510, 1465, 1378, 1293, 1200, 1152, 1028, 869, 866, 804, 720, 694, 635. Anal. Calcd for $(C_{85}H_{130}N_2O_4)_n$: C, 82.07; H, 10.53; N, 2.25. Found: C, 81.84; H, 10.41; N, 2.26.

**P5:** Black rubbery solid. Yield: 65%. $^1$H NMR ($CDCl_3$, $\delta$, ppm): 8.42 (s, 2H, Car), 7.79−7.48 (m, 4H, Car−H), 7.23 (m, 6H, Flu−H), 7.16 (m, 4H, Ar−H), 4.26 (b, 2H, Car−NC**H**$_2$−), 4.00 (b, 8H, ArOC**H**$_2$−), 1.73 (b, 8H, ArOCH$_2$**CH**$_2$−), 1.38−1.18 (b, 99H, −CH$_2$**(CH**$_2$**)**$_9$CH$_3$, −N(CH$_2$C**H**(CH$_3$)(**CH**$_2$)$_4$CH$_3$), Flu-(**CH**$_2$)$_5$CH$_3$), 0.91−0.80 (m, 18H, −**CH**$_3$). $^{13}$C NMR ($CDCl_3$, $\delta$, ppm): 150.5, 140.4, 139.9, 137.1, 132.1, 131.9, 131.8, 131.2, 129.3, 128.4, 128.3, 127.9, 127.5, 124.4, 123.0, 121.1, 119.1, 117.0, 116.7, 115.3, 108.2, 69.9, 55.0, 40.6, 39.5, 31.8, 31.6, 31.0, 30.1, 29.9, 29.5, 29.2, 28.8, 26.1, 24.4, 24.0, 23, 22.6, 14.0, 13.9, 10.9. FT-IR (KBr, cm$^{-1}$): 3464, 3054, 2924, 2853, 1865, 1606, 1511, 1465, 1378, 1294, 1200, 1120, 1045, 867, 805, 721, 695. Anal. Calcd for $(C_{106}H_{163}NO_2)_n$: C, 84.01; H, 10.84; N, 0.92. Found: C, 84.02; H, 10.59; N, 1.00.

## Results and Discussion

**Synthesis and Characterization:** The general synthetic route for the monomers and polymers **P1**−**P3** and **P4**−**P5** are outlined in Schemes 2 and 3, respectively. The monomer 1,4-bis (dodecyloxyphenyl)-2,5-diboronic acid (**4**) was synthesized from hydroquinone using a reported procedure.[34] 2,5-dibromohydroquinone (**2**) was obtained via bromination of hydroquinone with bromine in acetic acid.[35] Alkylation of **2** with dodecyl bromide in the presence of NaOH/EtOH gave compound **3**, which was reacted with *n*-butyllithium followed by quenching with triisopropyl borate and hydrolyzed with hydrochloric acid to afford bis(boronic acid) **4**. *N*-alkylated dibromocarbazoles (**7a**−**7c**) were synthesized from carbazole **5**. The carbazole was brominated with *N*-bromo succinimide (NBS) in DMF at room temperature to give the 3,6-dibromo carbazole (**6**).[27] The obtained dibromo compound was then alkylated with bromoalkanes in the presence of KOH in THF to afford the *N*-alkylated dibromocarbazoles (**7a**−**7c**).[17] All polymerizations were done using Suzuki polycondensation reactions using a mixture (2:3 v/v) of THF and aqueous potassium carbonate solution (2 M), containing 3.0 mol % $Pd(PPh_3)_4$ and stirred for 4 days at 70−80 °C under nitrogen atmosphere. About 40 mol % of CTAB was added to the reaction mixture as a phase transfer catalyst. For the polymers **P1**−**P3**, compound **4** and *N*-alkylated dibromocarbazoles (**7a**−**7c**) were used for the polymerization in the ratio of 1:1 while for **P4**−**P5**, the boronic acid **4**, *N*-alkylated dibromo carbazole (**7b**), and either 2,5-dibromopyridine (**8**) or alkylated dibromofluorene (**9**)[36] were used in a ratio of 1:0.5:0.5. After completion of the reaction, the polymers were precipitated from methanol. The resultant solid was suspended in acetone to remove impurities including oligomers and catalyst. Purified polymers were then filtered and reprecipitated from methanol.

**Table 1. Molecular Weight, Polydispersity Index, and Thermal Properties of the Polymers, P1−P5**

| polymer | color | $M_n$ | $M_w$ | PDI | onset, $T_d$ | $T_g$ |
|---|---|---|---|---|---|---|
| **P1** | black | 9850 | 14688 | 1.4 | 376, 486 | 112 |
| **P2** | black | 23117 | 32412 | 1.4 | 372, 504 | 116 |
| **P3** | black | 18581 | 24437 | 1.3 | 382 | 114 |
| **P4** | pale black | 11816 | 14879 | 1.2 | 390 | 96 |
| **P5** | grey black | 21965 | 30943 | 1.4 | 370 | 98 |

The molecular weights of the polymers were measured using gel permeation chromatography (GPC) with THF as eluant and polystyrene as the standard (Table 1). The obtained molecular weights were in the range of 15−33 kDa. Polymers, **P1**−**P5** were soluble in common organic solvents, such as THF, dichloromethane, chloroform, toluene and hexane and insoluble in polar solvents such as acetone and methanol. Full characterizations of the polymers (**P1**−**P5**) were achieved using FTIR, $^1$H NMR, $^{13}$C NMR, GPC, elemental analysis, TGA, and X-ray diffraction.

The assignments of the $^1$H and $^{13}$C NMR peaks are given in the Experimental Section. For polymer **P1,** the peaks at 8.42 (singlet), 7.78 (doublet) and 7.48 ppm (doublet) can be assigned to the carbazole protons and the one around 7.26 ppm could be

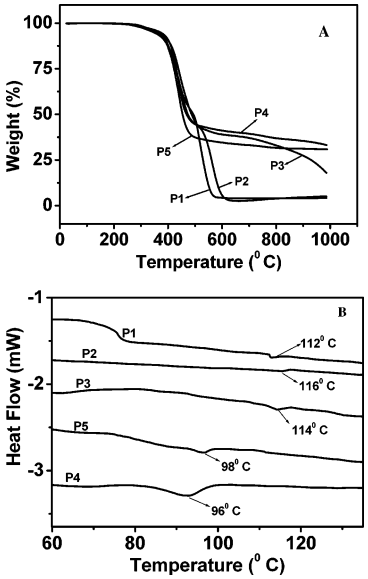


**Figure 1.** (A) TGA and (B) DSC traces of the polymers, **P1**−**P5**.

due to the aromatic protons. The peak at 4.37 ppm is due to the $-CH_2-$ protons of the *N*-hexyl group. The $-OCH_2-$ groups of the dialkyl benzene units appeared at 3.99 ppm, $-NCH_2\mathbf{CH}_2$ protons of the carbazole unit appeared at 1.96 ppm and the remaining peaks centered at 1.71, 1.36, and 1.15 ppm are assigned to the hydrogen atoms on the aliphatic dodecyloxy groups and the remaining $-CH_2$ protons of the *N*-hexyl group. The peaks at 0.9−0.8 ppm could be due to the $-CH_3$ groups of the alkyl chains. Data for polymers **P2**−**P5** were also in good agreement with their molecular structures (Scheme 1). From the $^1$H NMR spectrum of **P4**, the integration of aromatic protons of pyridine, carbazole and benzene are 3, 6, and 4, respectively. It confirmed that the distribution of pyridine and carbazole is about 25% each in the polymer backbone and the remaining 50% from the dialkoxy phenylene units. A similar result was obtained for the polymer **P5**. In addition to NMR spectra, the elemental analysis results of polymers **P1**−**P5** supported the proposed structures (please see the Supporting Information for the $^1$H NMR spectra with assignments). Thus, we confirm that the polymers (**P4** and **P5**) have the composition 0.5:0.5:1 of alkylated carbazole, pyridine (for **P4**) or dialkyl fluorene (for **P5**) and dialkoxybenzene, respectively.

**Thermal Properties.** Thermal properties of the polymers were investigated using thermogravimetric analysis (TGA) and differential scanning calorimetry (DSC) at a heating rate of 10 °C/min under nitrogen atmosphere. The polymers showed a small weight loss (<5%) below 300 °C which may be due to the trapped solvent in the polymer matrix. The degradation temperatures and $T_g$ values were tabulated in Table 1. The thermogram indicates that the polymers **P1**−**P5** are thermally stable up to 390 °C.

The first onset degradation temperatures were in the range of 380−400 °C (Figure 1A). The subsequent onset degradation temperature and weight loss of these materials were beyond 400 °C was proportional to the mass of their corresponding alkyl substituents as shown in Figure 1A. Degradation pathways depend on the number of alkyl chain substituents, which were decomposed very rapidly. In the case of polymers **P1**−**P2**, there was a second decomposition starting at 490 °C, which may due to the complete decomposition of the polymer backbone. However, in the case of polymers **P3**−**P5**, no further degradation or weight loss was observed up to 1000 °C. No significant changes in the decomposition temperature of the polymers were observed by incorporating pyridine or dialkylated fluorene on the polymer backbone. DSC thermograms of the polymers showed (Figure 1B) that the glass transition temperatures ranged from 96 to 116 °C. Higher the amount of carbazole content on the polymer backbone (**P1**−**P3**), the observed $T_g$ values were higher.

**Table 2. Absorption and Emission Wavelength for the Polymers P1−P5 in THF**

| | solution (THF) | | solid (film) | | | | |
|---|---|---|---|---|---|---|---|
| polymer | $\lambda_{max}$ (nm) | $\lambda_{em}$ (nm) | $\lambda_{max}$ (nm) | $\lambda_{em}$ (nm) | $\epsilon_{max}$ | band gap[a] | QE($\phi$)[b] |
| **P1** | 329 | 393 | 338 | 399, 424 | $3.55 \times 10^4$ | 3.28 | 0.58 |
| **P2** | 329 | 394 | 338 | 397, 421 | $3.55 \times 10^4$ | 3.27 | 0.62 |
| **P3** | 328 | 395 | 337 | 395, 418(s) | $3.32 \times 10^4$ | 3.26 | 0.61 |
| **P4** | 357 | 432 | 382 | 440, 464(s) | $4.98 \times 10^4$ | 2.96 | 0.78 |
| **P5** | 347 | 415 | 359 | 421, 437(s) | $6.26 \times 10^4$ | 3.09 | 0.72 |

[a] Calculated from the onset wavelength. [b] Measured using quinine sulfate as standards in THF.

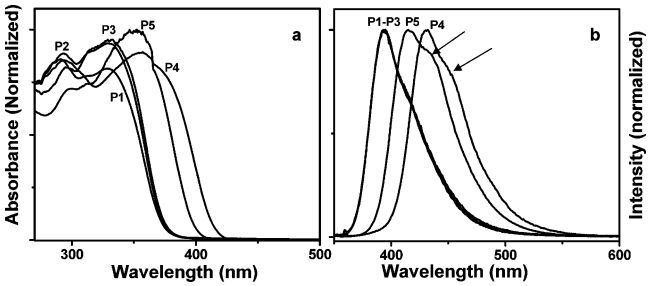


**Figure 2.** Absorption (a) and emission (b) spectra of the polymers **P1**−**P5** in THF; The concentration of the polymers **P1**−**P5** were $5.75 \times 10^{-5}$, $5.52 \times 10^{-5}$, $5.13 \times 10^{-5}$, $3.21 \times 10^{-5}$ and $3.99 \times 10^{-5}$ M, respectively (shoulders are indicated by arrows).

## Optical Properties

**Absorption and Emission Spectra.** The optical properties of the polymers **P1**−**P5** were measured both in solution and in thin films (Table 2). As expected, the optical properties of the polymers in tetrahydrofuran (THF) solution are dependent on the structure of the polymer backbone. The representative UV−vis absorption and fluorescence spectra of the polymers **P1**−**P5** in THF are given in Figure 2. Absorption spectra of these polymers showed two maxima ($\lambda_{max}$), one in the range 290−300 nm and another above 300 nm. For copolymers **P1**−**P3**, the absorption maxima were observed at 329, 328, and 329 nm, respectively, (Figure 2, Table 2). There were no significant changes in the $\lambda_{max}$ with changes in the length of alkyl chains. These values lie between those for homopolymers of 3,6-substituted carbazoles (308 nm) and dialkoxybenzene (370 nm).[18,37] Introduction of electron rich dialkoxybenzene units into the homopolymer of carbazole, increase the electron density of the polymer backbone as compared to polycarbazoles. This is consistent with the observed red shift in the $\lambda_{max}$ for **P4** (357 nm) and **P5** (347 nm) with decreasing carbazole contents. By introduction of 0.25 equiv of pyridine (for **P4**) or fluorene (for **P5**), red-shifts in $\lambda_{max}$ of 28 (**P4**) and 18 nm (**P5**) were observed, implying the extension of conjugation and incorporation of donor/acceptor system along the polymer backbone.

The band gap of the polymers **P1**−**P3** (3.28, 3.27, and 3.26 eV) are comparable with the corresponding homopolymer of 3,6-disubstituted carbazole (3.2 eV). Introduction of pyridine and fluorene units on the polymer backbone results in the reduction of band gap to 2.96 and 3.09 eV, for **P4** and **P5**, respectively. The presence of the fluorene unit in **P5** is responsible for the enhanced steric effect between dialkoxy-

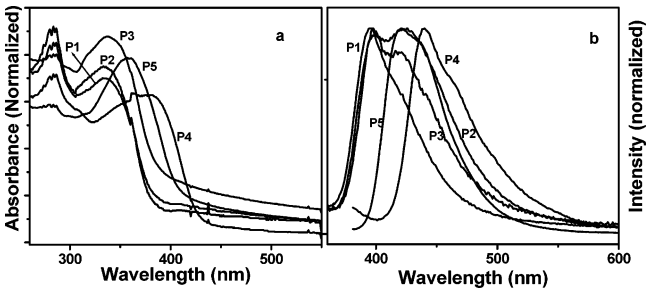


**Figure 3.** (a) Absorption and (b) Emission spectra of the polymers **P1**−**P5** in dip-casted thin film state.

benzene and fluorene backbone, which may lower the effective conjugation length in **P5** as compared to polymer **P4**.

The fluorescence spectra of the polymers were recorded with the excitation wavelength corresponding to their maximum absorption wavelength. The $\lambda_{em}$ of the polymers, **P1**−**P3**, **P4,** and **P5** are 338, 432, and 415 nm, respectively. The $\lambda_{em}$ values for the copolymers **P1**−**P3** were comparable with the polycarbazole as well as the alkoxylated poly(*p*-phenylene)s. There was a red shift observed when a third monomer (e.g., pyridine or fluorene) was incorporated on the polymer backbone. In the emission spectrum of **P4** and **P5** in dilute solution, there was a shoulder peak at around 449 and 434 nm (see arrows in Figure 2b). These shoulder peaks could be due to the emission of aggregates in dilute solution or localized conjugated segments along the polymer backbone.[38]

The fluorescence quantum efficiencies ($\phi_{fl}$) of the polymers were also measured in dilute THF solution using quinine sulfate ($\phi_{fl} = 0.55$ in 0.1 N $H_2SO_4$) as standard.[39,40] The quantum yields of the polymers **P1**−**P3** were in the range of 0.58−0.78, which was significantly higher than the polycarbazoles.[18a] Also for polymers **P4** and **P5**, the quantum yields were increased to 0.78 and 0.72, respectively. Incorporation of pyridine and fluorene resulted in the extension of conjugation of the backbone. As the conjugation length increases, the nonradiative decay rate decreases,[41] which result in the observed trend in quantum yield. Thus, the polymers are highly fluorescent which may be used for application in LED. The quantum yields of the polymers are listed in Table 2.

The transparent polymer thin films of all polymers (**P1**−**P5**) were fabricated on quartz plates by dip casting their solutions in THF (5 mg/mL) at room temperature. These films were subjected to both absorption and emission measurements (Figure 3) and showed bathochromic shifts of a few nanometers and broadening of the emission bands in comparison to their solution spectra. For the polymers **P1**−**P3**, a red shift of about 10 nm in the UV−vis spectra, 5 nm red shift in the emission spectra and significant shoulder peaks around 420 nm were observed. Similar red shifts were also observed for the polymers **P4** and **P5**. The significant shoulder peaks may due to the $\pi-\pi$ stacking or aggregation of the polymer chains. All spectral parameters are summarized in Table 2.

**Powder Diffraction Studies.** The XRD patterns of the powdered samples of polymers **P1**−**P5** were recorded to understand their self-assembly in the solid state. The X-ray patterns for the polymer powders (**P1**−**P5**) are given in Figure 4. For polymer **P2**, the peak appearing at a small angle region ($2\theta = 4.5°$) is assigned to the intermolecular distance between two main chains separated by the long alkyl chains. A similar lattice was also observed for the alkoxy-substituted $\pi$-conjugated polymers.[27,42−45] The observed distance of about 20.0 Å supports the interdigitation of alkyl chains.[42] In the case of polymers **P1** and **P3**−**P5**, no peaks were observed around 5° or lower. The peak around 21−22° (4.2 Å) for all the polymers is assigned to the face-to-face distance of inter polymer chain in the parallel packed lattice. Unfortunately, our machine does not allow us to measure the diffraction pattern below a value of $2\theta = 1.5°$ and small angle diffraction peaks are not visible in the X-ray diffraction pattern.

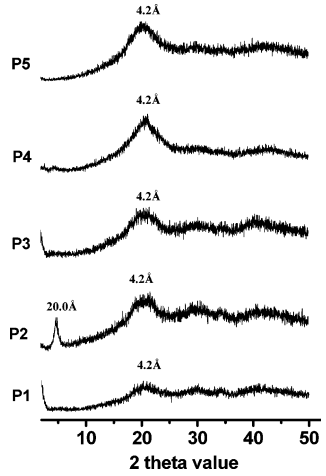


**Figure 4.** XRD powder patterns of the polymers **P1**−**P5.** The powder spectra were taken using powdered polymer samples placed on the sample pan.

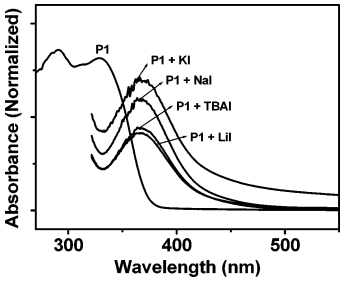


**Figure 5.** Absorption spectrum of **P1**, **P1**+Iodides. Concentration of **P1** is $5.75 \times 10^{-5}$ M.

**Iodide Sensing Studies.** Research on conjugated polymer-based sensors has attracted considerable attention in the recent years.[8] Selective chemosensors of anions such as fluoride,[46−50] nitrate,[51] and cyanide[52] based on small molecules and a few conjugated polymers[53−56] have been reported in the literature. Among the range of biologically important anions, iodide is of particular interest due to its essential role for thyroid gland function.[54] The sensing properties of the polymers **P1**−**P5** were studied in THF solutions using aliquots of methanolic/aqueous

**Table 3. Absorption and Emission Responses of P1−P5 upon Addition of Iodides**

| polymer | $\lambda_{max}/\lambda_{em}$ (nm) ($I^-$ free) | $\Delta\lambda_{max}/\Delta\lambda_{em}$ in the presence of iodides (nm) | | | | $K_{sv}$ upon addition of (TBA)I |
|---|---|---|---|---|---|---|
| | | (TBA)I | LiI | NaI | KI | |
| **P1** | 329/393 | 35/25 | 31/25 | 31/27 | 33/27 | $2.74 \times 10^4$ |
| **P2** | 329/394 | 35/26 | 32/33 | 33/33 | 35/30 | $3.17 \times 10^4$ |
| **P3** | 328/395 | 40/44 | 31/26 | 31/28 | 31/28 | $3.34 \times 10^4$ |
| **P4** | 357/432 | 16/20 | 4/8 | 4/7 | 4/8 | $1.43 \times 10^4$ |
| **P5** | 347/415 | 17/26 | 12/19 | 14/25 | 13/20 | $1.60 \times 10^5$ |

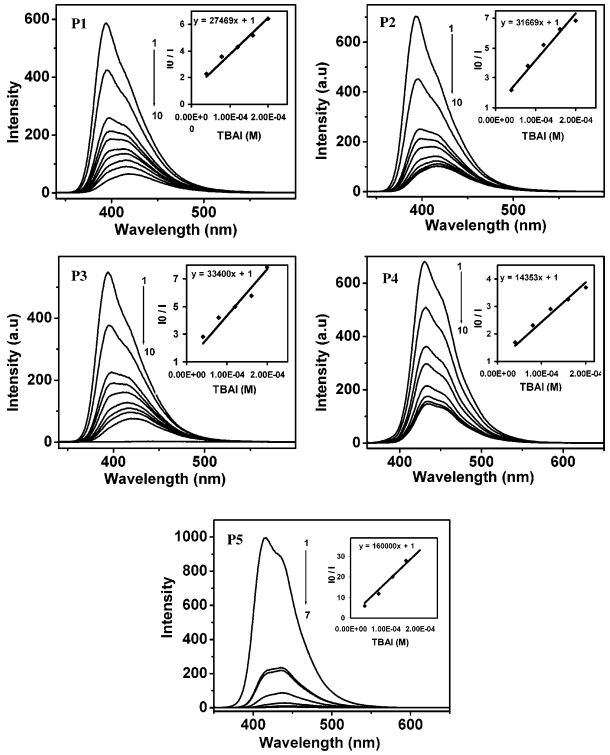


**Figure 6.** Changes in the emission spectra of **P1**−**P5** at different concentrations of (TBA)I (methanolic solution): For **P1**−**P4**, (1) 0 $\mu$M, (2) 0.4 $\mu$M (0 mts), (3) 0.4 $\mu$M (20 mts), (4) 0.4 $\mu$M (30 mts), (5) 0.8 $\mu$M (5 mts), (6) 0.8 $\mu$M (20 mts), (7) 1.2 $\mu$M, (8) 1.6 $\mu$M, (9) 2.0 $\mu$M, (10) 2.0 $\mu$M (30 mts). For **P5,** concentration of (TBA)I: (1) 0 $\mu$M, (2) 0.4 $\mu$M, (3) 0.4 $\mu$M (10 mts), (4) 0.8 $\mu$M, (5) 1.2 $\mu$M, (6) 1.6 $\mu$M. Inset shows the Stern−Volmer plots for the respective iodides. Please see Supporting Information for spectral data of other iodides.

solutions of the tetrabutylammonium halides or metal halides (Figure 5, Table 3). Interestingly, these polymers detect only iodides among other common anions such as fluorides, chlorides, bromides, perchlorates, nitrates, hydrogen phosphates, and hydrogen sulfates. The initial colorless solutions of the polymers change to yellow color on the addition of iodide salts. With increase in time, the intensity of the yellow color increases. The nature of cations such as tetrabutylammonium (TBA) to lithium/sodium/potassium ions does not influence the color changes. The addition of iodide salt to the polymers produced a red shift in the absorption and emission maxima of the polymers and observed $\Delta\lambda_{max}$ and $\Delta\lambda_{em}$ are given in Table 3. The difference in $\lambda_{max}$ is larger for all polymers (~31−40 nm) except **P4** (~4−17 nm). Figure 5 shows the influence of the addition of different iodides on the absorption spectra of polymer **P1**. The red-shift in the absorption and emission maxima can be explained through intermolecular charge-transfer complex between the carbazole moieties of the polymer backbone with the iodide ions. Among the polymers, **P1**−**P3** show larger red-shift in the absorption compared to **P4**−**P5**, which may be due to the lesser amount of carbazole moieties present in the polymers **P4**−**P5**.

Figure 6 displays the fluorescence titration spectra of the polymers **P1**−**P5** with the addition of tetrabutylammonium iodides. Upon addition of iodide salts, the emission intensity decreased significantly with a red shift of 44 nm (Table 3). In consistent with the UV spectra, the fluorescence measurements also showed a similar observation that the shift and quenching of the emission ($\Delta\lambda_{em}$) upon addition of (TBA)I for the polymers **P1**−**P3** and **P5** is larger than that of polymer **P4**.

**Fluorescence Quenching.** In general, fluorescence quenching happened through variety of mechanisms, like ground-state complexation,[57a] charge-transfer phenomena,[57b] electronic energy transfer,[57c,d] fluorescence resonance energy transfer (FRET),[57e−g] heavy atom effect,[57h] magnetic perturbations,[57i,j] etc. In this case, the charge-transfer complex via a "heavy-atom" effect is proposed. The "heavy-atom" interaction between the excited state of the polymer and the inorganic anion (iodides), lead to an enhancement of the spin−orbit coupling.[58,59] Here, the "heavy-atom" effect is caused by the formation of a weak, transient, probably charge-transfer complex between the carbazole moieties in the polymer backbone and the iodide ions.[60]

In addition, there are two types of quenching, one is static quenching through the formation of a complex and the other is the dynamic quenching due to the random collisions between the emitter and the quencher. In both quenching mechanisms, the electron/energy transfer is involved from the emitter to the quencher and each can be quantitatively described by the Stern−Volmer studies.[58] Dynamic quenching involves the deactivation of the polymer exciton through collisions with quencher molecules or ions in solution. The rate of quenching can be determined by using the slope of the Stern−Volmer plot and lifetime measurements. Conversely, the static quenching results from complexation of the analyte to the receptor sites, creating a new absorption, relaxation or energy transfer processes that favor nonradiative decay or through a new excitation/emission behavior. Using Stern−Volmer plots, the equilibrium constant for static quenching ($K_{sv}$) could be calculated and considered as the binding constants for the quencher−acceptor system.[57e]

The quenching effects of the polymer fluorescence in the presence of (TBA)I salts and other metal iodides have been investigated in detail. The addition of iodide salts into the polymer solution quenched the fluorescence intensities of the polymer. The fluorescence intensities are decreased much with increase in time and are constant after some particular time interval. For every addition of iodides, the intensities were

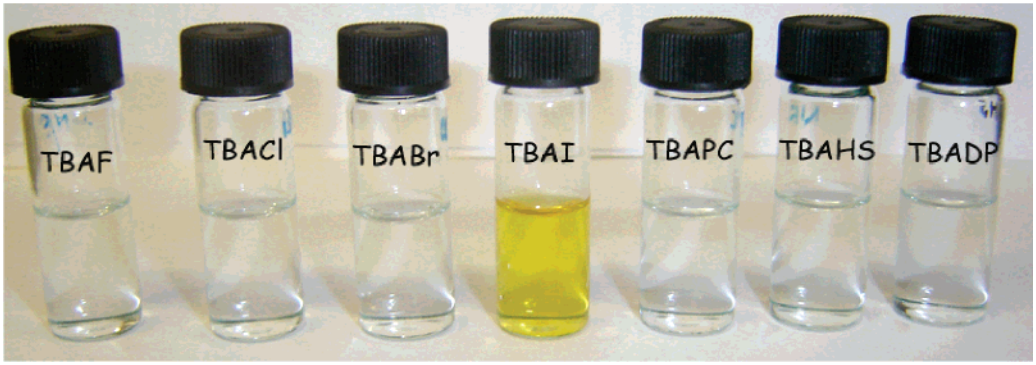


**Figure 7.** Color changes of polymer **P1** in THF upon addition of anion $F^-$ ((TBA)F), $Cl^-$ ((TBA)Cl), $Br^-$ ((TBA)Br), $I^-$ ((TBA)I), $ClO_4^-$ ((TBA)-PC), and hydrogen sulfate ((TBA)HS), $H_2PO_4^-$ ((TBA)DP). Concentration of **P1** and salt concentrations are $5.75 \times 10^{-5}$ M and 10 mM, respectively.

recorded for every 5 min until there was no change in intensities observed. The Stern−Volmer equation states that $I_0/I = 1 + K_{sv}$[quencher], where $I_0$ is the intensity of the fluorescence from the polymer in the absence of quencher and $I$ is the intensity in the presence of the quencher. $K_{sv}$ is the Stern−Volmer constant which provides the quantitative measure of the quenching. At low concentration of quenchers ((TBA)I), the quenching efficiency was more efficient and $I_0/I$ vs the concentration of the quencher gives a linear plot,[61] indicating a static quenching in which complex formation between polymer and quencher was observed. The Stern−Volmer constant $K_{sv}$ for all the polymers are tabulated in Table 3. Among the polymers **P1**−**P5**, the highest $K_{sv}$ values were obtained for **P5** by the addition of (TBA)I ($1.6 \times 10^5$) followed by the polymers, **P1**−**P3** (Table 3). The least $K_{sv}$ value is obtained for the polymer, **P4** ($1.4 \times 10^4$) which may be due to the presence of electron deficient pyridine moiety on the backbone.

Figure 7 shows a photograph of THF solutions of polymer **P1** containing anions $F^-$, $Cl^-$, $Br^-$, $I^-$, $ClO_4^-$, hydrogen sulfate ($HSO_3^-$), and $H_2PO_4^{2-}$ ((TBA)DP). Tetrabutylammonium was used as cation in all case. The solutions remained colorless upon addition of all the above anions except for $I^-$, where color changed to yellow. Hence, these polymers may be useful as colorimetric and fluorimetric sensors of iodide anions.

## Conclusion

A new series of copolymers consisting *N*-alkylated carbazole and dialkoxybenzene was successfully synthesized (**P1**−**P3**). The optical properties of these copolymers can be changed by changing the composition of the polymer backbone. Introduction of the pyridine and alkylated fluorene units on the polymer backbone of **P2** resulted in a red shift of 28 and 18 nm for **P4** and **P5**, respectively. There was a reduction in band gaps of polymers **P4** and **P5** (2.96 and 3.09 eV) compared to the carbazole−bis(dodecyloxy) benzene copolymers (3.26−3.28 eV). Thus, decrease in the amount of carbazole content along the polymer backbone increases the $\lambda_{max}$ and reduces band gaps. The molecular weights of these polymers were in the range of 15−33 kDa. These conjugated polymers were found to be thermally stable up to 390 °C and possessed good solubility, film-forming quality, thermal stability, optical properties and moderate quantum efficiencies. The sensing studies of these polymers were investigated by using the fluorescence quenching experiment by adding iodide salts and confirmed that these polymers may find useful applications in selective iodide identification colorimetrically as well as fluorimetrically. Such properties make these conjugated polymers promising candidates for advanced material such as sensors.

**Acknowledgment.** S.V. acknowledges the funding support from the National University of Singapore and the Agency for Science, Technology, and Research (ASTAR), Singapore. We thank the Singapore-MIT Alliance for research fellowships. The technical support from the Department of Chemistry, National University of Singapore, is also acknowledged. We thank the reviewers for their constructive comments and suggestions.

**Supporting Information Available:** Figures showing (1) $^1$H NMR spectra of the polymers (Figure 1a, $^1$H NMR spectra of the polymers **P1**−**P3**, with a and b = carbazole protons, c and d = aromatic protons, and e = Car−N−C**H**$_2$−, f = Ar−OC**H**$_2$−, and g = remaining aliphatic protons; Figure 1b, $^1$H NMR spectrum of polymer **P4**, with *a* = py−H, b = Car−H, c = py−H, d and e = Car−H, f = phenyl protons, g and h = Car−N−C**H**$_2$− and Ar−OC**H**$_2$−, i = remaining aliphatic protons; Figure 1c, $^1$H NMR spectrum of polymer **P5**, with a and b = Car−H, c = Flu−H, d = phenyl protons, e = Car−N−C**H**$_2$−, f = Ar−OC**H**$_2$−, and g = remaining aliphatic protons), (2) absorbance changes of the polymers, **P1**−**P5** by the addition of (TBA)I (Figure 2a, absorption spectrum of **P2**, **P2** + (TBA)I, where the concentration of **P2** was $5.52 \times 10^{-5}$ M; Figure 2b, absorption spectrum of **P3**, **P3** + (TBA)I, where the concentration of **P3** was $5.13 \times 10^{-5}$ M; Figure 2c, absorption spectrum of **P4**, **P4** + (TBA)I, where the concentration of **P4** was $3.21 \times 10^{-5}$ M; Figure 2d, absorption spectrum of **P5**, **P5** + (TBA)I, where the concentration of **P5** was $3.99 \times 10^{-5}$ M), (3) absorbance changes of the polymers, **P1**−**P5**, by the addition of LiI, NaI, and KI (Figure 3a, UV−vis absorption spectrum of **P2**, **P2** + iodides, where the concentration of **P2** was $5.52 \times 10^{-5}$ M; Figure 3b, UV−vis absorption spectrum of **P3**, **P3** + iodides, where the concentration of **P3** was $5.13 \times 10^{-5}$ M; Figure 3c, UV−vis absorption spectrum of **P4**, **P4** + iodides, where the concentration of **P4** was $3.21 \times 10^{-5}$ M; Figure 3d, UV−vis absorption spectrum of **P5**, **P5** + iodides, where the concentration of **P5** was $3.99 \times 10^{-5}$ M), and (4) fluorescence changes of the polymers, **P1**−**P5** by the addition of iodides (Figure 4a, changes in the emission spectra of **P1** at different concentrations of LiI, (1) 0, (2) 4, (3) 8, (4) 12, (5) 16, and (6) 24 mM, where the concentration of **P1** is $5.75 \times 10^{-5}$ M; Figure 4b, changes in the emission spectra of **P1** at different concentrations of NaI, (1) 0, (2) 4, (3) 8, (4) 16, and (5) 24 mM, where the concentration of **P1** is $5.75 \times 10^{-5}$ M; Figure 4c, changes in the emission spectra of **P1** at different concentrations of KI, (1) 0, (2) 4, (3) 8, and (4) 16 mM, where the concentration of **P1** is $5.75 \times 10^{-5}$ M; Figure 4d, changes in the emission spectra of **P2** at different concentrations of LiI (methanolic solution), (1) 0, (2) 4, (3) 8, (4) 12, (5) 16, and (6) 24 mM, where the concentration of **P2** was $5.52 \times 10^{-5}$ M; Figure 4e, changes in the emission spectra of **P2** at different concentrations of NaI (methanolic solution), (1) 0, (2) 4, (3) 8, (4) 16, and (5) 24 mM, where the concentration of **P2** was $5.52 \times 10^{-5}$ M; Figure 4f, changes in the emission spectra of **P2** at different concentrations of KI (methanolic solution), (1) 0, (2) 4, (3) 12, and (4) 16 mM, where the concentration of **P2** was $5.52 \times 10^{-5}$ M; Figure 4g, changes in the emission spectra of **P3** at different concentrations of LiI (methanolic solution), (1) 0, (2) 4, (3) 8, (4) 12, (5) 16, (6) 24, (7) 28, and (8) 32 mM, where the concentration of **P2** was $5.13 \times 10^{-5}$ M; Figure 4 h, changes in the emission spectra of **P3** at different concentrations of NaI (methanolic solution), (1) 0, (2) 4, (3) 8, (4) 12, (5) 16, and (6) 24 mM, where the concentration of **P3** was $5.13 \times 10^{-5}$ M; Figure 4i, changes in the emission spectra of **P3** at different concentrations of KI (methanolic solution), (1) 0, (2) 4, (3) 8, (4) 12, (5) 16, (6) 24, and (7) 28 mM, where the concentration of **P3** was $5.13 \times 10^{-5}$ M; Figure 4j, changes in the emission spectra of **P4** at different concentrations of LiI (methanolic solution), (1) 0, (2) 4, (3) 8, (4) 12, and (5) 16 mM, where the concentration of **P4** was $3.21 \times 10^{-5}$ M; Figure 4K, changes in the emission spectra of **P4** at different concentrations of NaI (methanolic solution), (1) 0, (2) 4, (3) 8, (4) 12, and (5) 16 mM, where the concentration of **P4** was $3.21 \times 10^{-5}$ M; Figure 4l, changes in the emission spectra of **P4** at different concentrations of KI (methanolic solution), (1) 0, (2) 4, (3) 8, (4) 12, and (5) 16 mM, where the concentration of **P4** was $3.21 \times 10^{-5}$ M; Figure 4m, changes in the emission spectra of **P5** at different concentrations of LiI (methanolic solution), (1) 0, (2) 4, (3) 8, (4) 12, (5) 16, (6) 20, and (7) 24 mM, where the concentration of **P5** was $3.99 \times 10^{-5}$ M; Figure 4n, changes in the emission spectra of **P5** at different concentrations of NaI (methanolic solution), (1) 0, (2) 4, (3) 8, (4) 12, (5) 16, and (6) 20 mM, where the concentration of **P5** was $3.99 \times 10^{-5}$ M; Figure 4o, changes in the emission spectra of **P5** at different concentrations of KI (methanolic solution), (1) 0, (2) 4, (3) 8, (4) 12, (5) 16, and (6) 20 mM, where the concentration of **P5** was $3.99 \times 10^{-5}$ M. This material is available free of charge via the Internet at http://pubs.acs.org.

## References and Notes


(1) Müllen, K.; Wegner, G. *Electronic Materials: The Oligomer Approach*; Wiley-VCH: Weinheim, Germany, 1998.
(2) *Handbook of Conducting Polymers*; Skotheim, T. A., Elsenbaumer, R. L., Reynolds, J. R., Eds.; Marcel Dekker: New York, 1997.
(3) Li, Z. L.; Yang, S. C.; Meng, H. F.; Chen, Y. S.; Yang, Y. Z.; Liu, C. H.; Horng, S. F.; Hsu, S.; Chen, L. C.; Hu, J. P.; Lee, R. H. *Appl. Phys. Lett.* **2004**, *84*, 3558−3560.
(4) Kraft, A.; Grimsdale, A. C.; Holmes, A. B. *Angew. Chem., Int. Ed.* **1998**, *37*, 403−428.
(5) Friend, R. H.; Gymer, R. W.; Holmes, A. B.; Burroughes, J. H.; Marks, R. N.; Taliani, C.; Bradley, D. D. C.; Dos Sontos, D. A.; Brédas, J. L.; Lögdlund, M.; Salaneck, W. R. *Nature* **1999**, *397*, 121−128.
(6) Bunz, U. H. F. *Chem. Rev.* **2000**, *100*, 1605−1644 and references cited therein.
(7) Peng, Q.; Lu, Z. Y.; Huang, Y.; Xie, M. G.; Xiao, D.; Han, S. H.; Peng, J. B.; Cao, Y. *J. Mater. Chem.* **2004**, *14*, 396−401.
(8) McQuade, D. T.; Pullen, A. E.; Swager, T. M. *Chem. Rev.* **2000**, *100*, 2537−2574.
(9) Gong, X.; Matthew, R. R.; Ostrowski, J. C.; Moses, D.; Bazan, G. C.; Heeger, A. J. *Adv. Mater.* **2002**, *14*, 581−585.
(10) Tour, J. M. *Acc. Chem. Res.* **2000**, *33*, 791−804.
(11) Yu, G.; Gao, J.; Hummelen, J. C.; Wudl, F.; Heeger, A. J. *Science* **1995**, *270*, 1789−1791.
(12) Yao, Y.; Lamba, J. J. S.; Tour, J. M. *J. Am. Chem. Soc.* **1998**, *120*, 2805−2810.
(13) Godt, A.; Schluter, A. D. *Adv. Mater.* **1991**, *3*, 497−499.
(14) Roncali, J. *Chem. Rev.* **1997**, *97*, 173−206.
(15) Morin, J. F.; Drolet, N.; Tao, Y.; Leclerc, M. *Chem. Mater.* **2004**, *16*, 4619−4626.
(16) Tschida, A.; Nagata, A.; Yamamoto, M.; Fukui, A.; Sawamoto, M.; Higashimura, T. *Macromolecules* **1995**, *28*, 1285−1289.
(17) Ostraukaite, J.; Strohriegl, P. *Macromol. Chem. Phys.* **2003**, *204*, 1713−1718.
(18) (a) Iraqi, A.; Wataru, I. *J. Polym. Sci. Part. A Polym. Chem.* **2004**, *42*, 6041−6051. (b) Iraqi, A.; Wataru, I. *Chem. Mater.* **2004**, *16*, 442−448. (c) Zhang, Z. B.; Fujiki, M.; Tang, H. Z.; Motonaga, M.; Torimitsu, K. *Macromolecules* **2002**, *35*, 1988−1990. (d) Witker, D.; Reynolds, J. R. *Macromolecules* **2005**, *38*, 7636−7644. (e) Huang, J.; Niu, Y.; Yang, W.; Mo, Y.; Yuan, M.; Cao, Y. *Macromolecules* **2002**, *35*, 6080−6082. (f) Wong, W. Y.; Liu, L.; Cui, D.; Leung, L. M.; Kwong, C. F.; Lee, T. H.; Ng, H. F. *Macromolecules* **2005**, *38*, 4970−4976. (g) Li, Y.; Ding, J.; Day, M.; Tao, Y.; Lu, J. D'iorio. *Chem. Mater.* **2004**, *16*, 2165−2173. (h) Pan, X. Y.; Liu, S.; Chan, H. S. O.; Ng, S. C. *Macromolecules* **2005**, *38*, 7629−7635.
(19) (a) Sigwalt, P.; Wegner, G.; Morin, J. F.; Leclerc, M.; Ades, D.; Siove, A. *Macro. Rapid. Com.* **2005**, *26*, 761−778. (b) Belletete, M.; Bouchard, J.; Leclerc, M.; Durocher, G. *Macromolecules* **2005**, *38*, 880−887. (c) Morin, J. F.; Boudreault, P. L.; Leclerc, M. *Macromol. Rapid. Com.* **2002**, *23*, 1032−1036. (d) Morin, J. F.; Leclerc, M. *Macromolecules* **2002**, *35*, 8413−8417. (e) Morin, J. F.; Leclerc, M. *Macromolecules* **2001**, *34*, 4680−4682.
(20) Kuwabara, Y.; Ogawa, H.; Inada, H.; Nona, N.; Shirota, Y. *Adv. Mater.* **1994**, *6*, 667−669.
(21) O'Brien, D. F.; Burrows, P. E.; Forrest, S. R.; Koene, B. E.; Loy, D. E.; Thompson, M. E. *Adv. Mater.* **1998**, *10*, 1108−1112.
(22) Koene, B. E.; Loy, D. E.; Thompson, M. E. *Chem. Mater.* **1998**, *10*, 2235−2250.
(23) Thomas, K. R. J.; Lim, J. T.; Tao, Y. T.; Ko, C. W. *J. Am. Chem. Soc.* **2001**, *123*, 9404−9411.
(24) Li, J.; Liu, D.; Li, Y.; Lee, C. S.; Kwong, H. L.; Lee, S. *Chem. Mater.* **2005**, *17*, 1208−1212.
(25) Liu, B.; Yu, W. L.; Lai, Y. H.; Huang, W. *Chem. Mater.* **2001**, *13*, 1984−1991.
(26) Xia, C.; Advincula, R. C. *Macromolecules* **2001**, *34*, 5854−5859.
(27) Stephen, O.; Vial, J.-C. *Synth. Met.* **1999**, *106*, 115−119.
(28) Baskar, C.; Lai, Y. H.; Valiyaveettil, S. *Macromolecules* **2001**, *34*, 6255−6260 and references cited therein.
(29) Ji, W.; Elim, H. I.; He, J.; Fitrilawati, F.; Baskar, C.; Valiyaveettil, S.; Knoll, W. *J. Phys. Chem. B* **2003**, *107*, 11043−11047.
(30) Renu, R.; Valiyaveettil, S.; Baskar, C.; Putra, A.; Fitrilawati, F.; Knoll, W. *MRS Proc.* **2003**, *776*, 201−202.
(31) Vetrichelvan, M.; Valiyaveettil, S. *Chem.—Eur. J.* **2005**, *11*, 5889−5898.
(32) Vetrichelvan, M.; Valiyaveettil, S. *Polym. Mater. Sci., Eng.* **2004**, *91*, 1033−1034.
(33) (a) Vetrichelvan, M.; Li, H.; Renu, R.; Valiyaveettil, S. *J. Polym. Sci., A: Polym. Chem.* **2006**, *44*, 3763−3777. (b) Vetrichelvan, M.; Li, H.; Valiyaveettil, S. *Polym. Prepr.* **2005**, *46*, 104.
(34) Aubert, P. H.; Knipper, M.; Groenendaal, L.; Lutsen, L.; Manca, J.; Vanderzande, D. *Macromolecules* **2004**, *37*, 4087−4098.
(35) Tietze, L. F.; Eicher, Th. *Reactions and Syntheses in the Organic Chemistry Laboratory*, University Science: Mill Valley, CA, 1989; p 253.
(36) Lee, J.; Cho, H. J.; Jung, B. J.; Cho, N. S.; Shim, H. K. *Macromolecules* **2004**, *37*, 8523−8529.
(37) Vahlenkamp, T.; Wegner, G. *Macromol. Chem. Phys.* **1994**, *195*, 1933−1952.
(38) Wu, T. Y.; Chen, Y. *J. Polym. Sci. Part. A Polym. Chem.* **2002**, *40*, 3847−3857.
(39) Joshi, H. S.; Jamshidi, R.; Tor, Y. *Angew. Chem., Int. Ed. Engl.* **1999**, *38*, 2721−2725.
(40) Demas, J. N.; Grosby, G. A. *J. Phys. Chem.* **1971**, *75*, 991−1024.
(41) Warmser, C. C. *Spectrum* **1998**, *11*, 1−12.
(42) Yamamoto, T.; Fang, Q.; Morikita, T. *Macromolecules* **2003**, *36*, 4262−4267.
(43) McCullough, R. D.; Tristam-Nagle, S.; Williams, S. P.; Lowe, R. D.; Jayaraman, M. *J. Am. Chem. Soc.* **1993**, *115*, 4910−4911.
(44) Chen, T.-A.; Wu, X.; Rieke, R. D. *J. Am. Chem. Soc.* **1995**, *117*, 233−244.
(45) Yamamoto, T.; Komarudin, D.; Arai, M.; Lee, B.-L.; Suganuma, H.; Asakawa, N.; Inue, Y.; Kubata, K.; Sasaki, S.; Fukuda, T.; Watsuda, H. *J. Am. Chem. Soc.* **1998**, *120*, 2047−2058.
(46) Curiel, D.; Cowley, A.; Beer, P. D. *Chem. Commun.* **2005**, 236−237.
(47) Cooper, C. R.; Spencer, N.; James, T. D. *Chem. Commun.* **1998**, 1365−1366.
(48) Jursikova, K.; Sessler, J. L. *J. Am. Chem. Soc.* **2000**, *122*, 9350−9351.
(49) Black, C. B.; Andrioletti, B.; Try, A. C.; Ruiperez, C.; Sessler, J. L. *J. Am. Chem. Soc.* **1999**, *121*, 10438−10439.
(50) Tong, H.; Wang, L.; Jing, X.; Wang, F. *Macromolecules* **2003**, *26*, 2584−2586.
(51) Sancenon, F.; Manez, R. M.; Soro, J. *Angew. Chem., Int. Ed.* **2002**, *41*, 1416−1419.
(52) Anzenbacher, P.; Tyson, D. S.; Jursikova, K.; Castellano, F. N. *J. Am. Chem. Soc.* **2002**, *124*, 6232−6233.
(53) Zhou, G.; Cheng, Y.; Wang, L.; Jing, X.; Wong, F. *Macromolecules* **2005**, *38*, 2148−2153.
(54) (a) Ho, H. A.; Leclerc, M. *J. Am. Chem. Soc.* **2003**, *125*, 4412−4413. (b) Kim, T.-H.; Swager, T. M. *Angew. Chem., Int. Ed.* **2003**, *42*, 4803−4806.
(55) Brockmann, T. W.; Tour, J. M. *J. Am. Chem. Soc.* **1995**, *117*, 4437−4447.
(56) Yao, Y.; Zhang, Q. T.; Tour, J. M. *Macromolecules* **1998**, *31*, 8600−8606.
(57) (a) Rutter, W. J. *Acta Chem. Scand.* **1958**, *12*, 438. (b) Hariharan, C.; Vijaysree, V.; Mishra, A. K. *J. Lumin.* **1997**, *75*, 205−211. (c) Bregadze, V.; Khutsishvili, I.; Chkhaberidze, J.; Sologhashvili, K. E. *Inorg. Chim. Acta* **2002**, *339*, 145−159. (d) Guarino, A.; Possagno, E.; Bassanelli, R. *J. Chem. Soc., Faraday Trans.1* **1980**, *76*, 2003−2010. (e) Murphy, C. B.; Zhang, Y.; Troxler, T.; Ferry, V.; Martin, J. J.; Jones, W. E., Jr. *J. Phys. Chem. B.* **2004**, *108*, 1537−1543. (f) Zheng, J.; Swager, T. M. *Chem. Commun.* **2004**, *24*, 2798−2799. (g) Kim, J.; McQuade, T.; Rose, A.; Zhu, Z.; Swager, T. M. *J. Am. Chem. Soc.* **2001**, *123*, 11488−11489 (g) (h) Lower, S. K.; El-Sayed, M. A. *Chem. Rev.* **1966**, *66*, 199−241. (i) Yuster, P.; Weissman, S. I. *J. Chem. Phys.* **1949**, *17*, 1182−1188.
(58) Lakowicz, J. R. *Principles of Fluorescence Spectroscopy*, 2nd ed.; Plenum Press: New York, 1999.
(59) (a) Watkins, A. R. *J. Phys. Chem.* **1974**, *78*, 1885−1890. (b) Kasha, M. *J. Chem. Phys.* **1952**, *20*, 71−74.
(60) McGlynn, S. P.; Azumi, T.; Khinoshita, M. *Molecular Spectroscopy of the Triplet State*; Prientice-Hall: Englewood Cliffs, NJ, 1969; pp 40−43.
(61) Wang, J.; Wang, D.; Miller, E. K.; Moses, D.; Bazan, G. C.; Heeger, A. J. *Macromolecules* **2000**, *33*, 5153−5158.


MA0613537